Nigerian Journal of Engineering, Vol. 29, No. 1, April 2022, ISSN (print): 0794 – 4756, ISSN(online):2705-3954.

Nigerian Journal of Engineering,
Faculty of Engineering, Ahmadu Bello University, Zaria, Nigeria
journal homepage: www.njeabu.com.ng

A Comparative Study of Iterative and Non-Iterative Load-Flow Methods: A Case of Newton-Raphson and Holomorphic Embedding Approaches

F. Olobaniyi*, O. Oparinde, O. Ogundipe

Department of Electrical and Electronics Engineering, University of Lagos, Yaba, Lagos – Nigeria.
*folobaniyi@unilag.edu.ng

Research Article

Abstract

Given the crucial role load flow analysis plays in the planning and operation of power systems, there is a growing requirement to produce load flow methods that would perform with unerring accuracy and also be free from the convergence concerns associated with the classical iterative methods. The Holomorphic Embedding Load-flow Method (HELM) is one of such attempts. It is non-iterative and could produce a solution when it is available and indicate when there is no solution to signal an abnormality, such as a voltage collapse. According to literature, the Newton-Raphson load flow method (NRLM) is the most widely utilized iterative method due to its remarkable qualities, therefore it is the preferred choice here for comparison. The objective of this paper is to weigh up the merits of HELM over the NRLM based on information obtained from actual applications and since HELM is not found as one of the methods previously applied for the analysis of the Nigerian network, the behaviour of the system with HELM is assessed. Analyses of particular systems were done at least three times and the average time for each was computed. HELM was found to be faster by a wide margin in all the cases. For example, HELM was 95.7% faster than the NRLM for the 4-bus system and 80.6% faster when applied to the Nigerian 330kV transmission network. This validates a major advantage of HELM over iterative solutions. However, the node voltages of Nigerian system were not as close as results for standard IEEE systems which can be attributed to the condition of the network which HELM, as one of its advantages is believed to expose. Secondly, though the special software produced for HELM analyses might be the best for it, an attempt was made to adapt to a MATLAB program since the software is easily accessible. More work is required in the programming to successfully analyse large and ill-conditioned systems.

Keywords
Approximants; holomorphicity; holomorphic embedding load flow; newton-raphson load flow

Article History
Received: – October, 2020
Reviewed: – March, 2021
Accepted: – May, 2022
Published: – April, 2022

1. Introduction

Load flow analysis is of paramount importance in the successful operation of an existing power system while providing a platform for reliable planning processes, therefore, accurate load-flow results are critical (Theraja & Theraja, 2012; Mehta, Mohlzahn, & Turitsyn, 2016; Metha & Metha, 2017). The main classical iterative load flow methods are the Gauss-Seidel load flow method (GSLM), Newton-Raphson load flow method (NRLM), Fast Decoupled Load Flow (FDLF), and their variants. Other methods include Fuzzy Logic, Genetic Algorithm application, and the Particle swarm method. The NRLM is the most commonly used because it provides the best characteristics of quadratic convergence in a minimum number of iterations (Subramanian, 2014; Rao, 2016; Trias, 2015) and is well suited for the Nigerian system (Onojo et al., 2013; Olobaniyi, 2015)

1.1 Basic Concepts of Load Flow Analysis

The load-flow study is a numerical analysis of the flow of electric power in an interconnected system. The procedure and outcomes are summarized in Figure 1, where the voltage at each bus and the real and reactive power flow in normal steady-state operation are the principal output. It uses simplified notation such as a one-line diagram and the per-unit system.

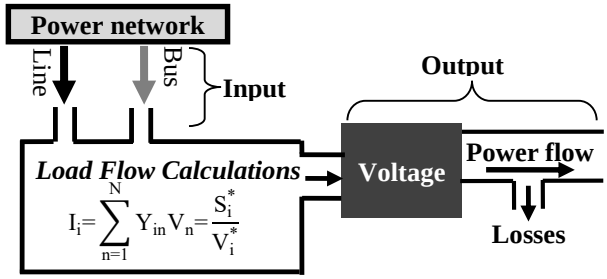

Figure 1: General concept of load flow analysis

1.2 Power Flow Equations

Generally, the load flow within an a.c. power system is done by solving typical power flow equations for the system and this begins by identifying the bus types as generator bus, load bus, and slack bus based on their functions and the known quantities. The buses are associated with four quantities - magnitude and

phase angle of voltage, active and reactive power. Any two of these are specified at each bus and the remaining two are to be determined. The set of equations representing the power system can be written in the following general form:

$$S_i = V_i I_i^* \quad (i=1, 2, \ldots, N) \tag{1}$$

where N is the total number of buses, *I* is any node or bus in the system and I_i is the sum of currents of all other nodes that physically connect to *i* represented by equation (2). Where Y_{in} is the admittance of the line connecting bus, *i* and another bus, *n*; V_n is the voltage at bus *n* and S_i is the complex power at bus *i*, also separated into the active power, P_i and reactive power, Q_i. From this, **Error! Reference source not found.** and **Error! Reference source not found.** are obtained.

$$I_i = \sum_{n=1}^{N} Y_{in} V_n = \frac{S_i^*}{V_i^*} = \frac{P_i - jQ_i}{V_i^*} \quad (i=1, 2, \ldots, N) \tag{2}$$

$$P_i - \sum_{n=1}^{N} |V_i V_n Y_{in}| \cos(\delta_i - \delta_n - \theta_{in}) \tag{3}$$

$$Q_i - \sum_{n=1}^{N} |V_i V_n Y_{in}| \sin(\delta_i - \delta_n - \theta_{in}) \tag{4}$$

This is the system of nonlinear equations usually solved to find the solution of the load flow analysis. The major challenge is getting accurate load flow results all the time because a nonlinear system may have more than one equilibrium point. This is responsible for the continuous search for better analysis methods which include iterative, non-iterative and hybrid methods.

1.3 Non-iterative Methods versus Iterative Methods of Load Flow Analysis

The series load flow method proposed by (Sauer, 1981) and extended by (Xu, W., et al, 1998) uses Taylor's series expansion around a feasible operating point and is non-iterative. The sensitivity of voltages to bus power injections could be determined directly but applies analytic representation of the process rather than the original Power Balance Equations (PBE's) which is impractical to obtain for large systems. Also, the initial operating point has to be obtained using an iterative approach and necessarily requires the factorization of matrices. Iterative methods are simpler, and since no full factorization has to be stored, much larger systems can be handled. Besides, high-level parallelism is easier to achieve with iterative solvers than with direct solvers (Cai & Mitra, 2012; Kalantari, et al, H., 2003). But fundamental problems have been identified with iterative methods which include the existence of real solutions and their semblances, a tendency for ill-conditioning, and convergence difficulties, especially in large-scale power systems (Huneault & Galiana, 1991; Trias, 2015) Divergence, or convergence to a non-operating solution, tends to occur especially at a point in the system close to a voltage collapse (Gupta, 2013; Hiskens 2003). A need, therefore, arises for load-flow methods that are devoid of these issues which have led to the development of the Holomorphic Embedding Load-flow method (HELM) (Black, 2012; Trias, 2012) which is completely non-iterative. It is reputed to find the operational voltage solution when it exists and indicates when the solution does not exist and is therefore particularly suited for real-time applications. Though HELM solves the convergence issues, it is based on complex analysis - holomorphic functions, Taylor's series, Padé approximants, convolution, and linear matrix equations which make it difficult to understand.

Though several load flow analyses have been conducted on the Nigerian 330kV system using well-known methods, some of which are reported in (Adejumobi et al. 2013; ; Ogbuefi et al, 2015; Ogujor et al 2012; Onohaebi & Apeh, 2007; Onojo, 2013; Samuel, 2014), literature could not be found that shows the application of HELM to the system. This work, therefore, sets out to find out the behaviour of the system with HELM compared to NRLM but starting by the application to the IEEE 4-bus system (Subramanian, 2014) to gain first-hand knowledge of the unique qualities of HELM.

2. Methodology

The NRLM and HELM are applied to a 4-bus system, the IEEE 14-bus, 30-bus and the Nigerian 330kV system following the steps below, though not strictly.

2.1 Solution Steps in NRLM

The Newton-Raphson method is a powerful technique for solving equations numerically and the steps are:

2.1.1 Identification of bus types

In any network, independent of the method of analysis, the types of buses are first identified. Four variables are associated with the buses - active power P, reactive power Q, voltage magnitude, |V| and voltage angle, δ. Two of these variables are specified at each bus and help to identify the buses as load, generator bus and the slack bus or swing bus, so-called because of its major function. The phase angles of other buses are expressed using the swing bus voltage phasor as a reference.

2.1.2 Formation of bus admittance matrix

The admittance matrix (Ybus) plays a key role and is formed using the line data and the dimension of the matrix depends on the number of buses in the network. Through the Ybus, the, the topology of the network can be understood at a glance and from it the amount of current at a bus, line flows and losses can be calculated. The elements can be computed from (5) and (6), where Y_{ii} represents the diagonal elements and Y_{in} the off-diagonal elements of the matrix.

$$Y_{ii} = \sum_{n \neq 1}^{N} y_{in} \tag{5}$$

$$Y_{in} = Y_{ni} = -y_{in} \tag{6}$$

2.1.3 Calculation of the initial values of power

The powers, P and Q are specified or estimated, and initial values of |V| and δ are chosen for each bus except the swing bus which they are known. These are used based on equations (5) and (6) to obtain the calculated values for the powers, as in (7) and (8), where *k* denotes the number of iterations.

$$P_i^{cal(k)} = \sum_{n=1}^{N} |V_i V_n Y_{in}| \cos(\theta_{in} - \delta_i - \delta_n) \quad (7)$$

$$Q_i^{cal(k)} = -\sum_{n=1}^{N} |V_i V_n Y_{in}| \sin(\theta_{in} - \delta_i - \delta_n) \quad (8)$$

2.1.4 Checking power mismatch

The differences between the specified and calculated values are shown in (9) and (10). The subscripts *sch* and *cal* are used for specified and calculated values respectively. The initial value for $P_i^{(sch)}$ is the specified P at the respective buses. After each iteration, the $P_i^{(sch)(k)}$ would be the previous $P_i^{(k)}$.

$$\Delta P_i^{(k)} = P_i^{(sch)(k)} - P_i^{(cal)(k)} \quad (9)$$

$$\Delta Q_i^{(k)} = Q_i^{(sch)(k)} - Q_i^{(cal)(k)} \quad (10)$$

2.1.5 Determining the elements of the Jacobian

In a concise form, the NRLM load flow method can be represented by (11), where the matrix $\mathbf{J}^{(k)}$ is called the Jacobian of the initial estimates represented by (12) and the variables with Δ are the differences. The elements of the Jacobian matrix are partial derivatives of P and Q with respect to |V| or δ. The calculation of each Jacobian element is required for each iteration.

$$\begin{bmatrix} \Delta P^{(k)} \\ \Delta Q^{(k)} \end{bmatrix} = \left[J^{(k)}\right] \begin{bmatrix} \Delta \delta^{(k)} \\ \Delta |V|^{(k)} \end{bmatrix} \quad (11)$$

$$\mathbf{J} = \begin{bmatrix} \frac{\partial P}{\partial \delta} & \frac{\partial P}{\partial V} \\ \frac{\partial Q}{\partial \delta} & \frac{\partial P}{\partial V} \end{bmatrix} = \begin{bmatrix} J_1 & J_2 \\ J_3 & J_4 \end{bmatrix} \quad (12)$$

2.1.6 Obtaining new estimates for voltage magnitude and voltage angle

The solution of the matrix equation (11) gives $\Delta\delta^{(k)}$ and $\Delta|V|^{(k)}$. A better estimate of the solution is expressed in (13) and (14).

$$\delta_i^{(k+1)} = \delta_i^{(k)} - \Delta\delta_i^{(k)} \quad (13)$$

$$\left|V_i^{(k+1)}\right| = \left|V_i^{(k)}\right| - \left|\Delta V_i^{(k)}\right| \quad (14)$$

The search for the best estimate or iteration is continued until the power mismatches are equal to or less than a tolerance value; the load flow is then said to have converged.

2.2 Solution Steps in HELM

HELM is a fairly recent method compared to other methods and it is non-iterative. The first two solutions steps in NRLM also apply to HELM; the other steps can be outlined as follows:

2.2.1 Choosing a suitable embedding complex parameter

If the chosen parameter is ***s***, the complex voltage variable is embedded as $V_i^*(s^*)$ to ensure holomorphicity.

2.2.2 Classifying functions

The embedded parameters define an algebraic curve and therefore the variable can be classified as holomorphic functions. The reference solution should be selected at s=0, but once solved, the reflection condition at s=1, should be requested. This represents only the feasible branches of the power flow problem while others are ghost branches.

2.2.3 Obtaining the system of equations

The original power balance equations are embedded with a complex variable, *s*, to yield the holomorphic embedded equations for the slack bus, load bus and generator bus of equations (15) - (37) (Subramanian *et al.*, 2015). The resulting system of equations consists of polynomials and by the application of Grobner basic theory; an equation in one variable can be obtained, say, $V_1(s)$, while the rest, including $\tilde{V}_n(s)$ may be obtained in a triangular form.

$$V_{slack}(s) = 1 + s\left(V_i^{sp} - 1\right) \quad (15)$$

$$\sum_{n=1}^{N} Y_{\text{in trans}} V_n(s) = \frac{sS_i^*}{V_i^*(S^*)} - sY_{ishunt} V_{i(s)} \quad (26)$$

$$\sum_{n=1}^{N} Y_{\text{in trans}}\, V_n s = \frac{s(P_i + jQ_i)(s)}{V_i^*(s^*)} - sY_{\text{ishunt}}\, V_i(s)$$
$$V_i(s)^* V_i^*(s^*) = 1 + s\left(\left|V_i^{sp}\right|^2 - 1\right) \quad (37)$$

2.2.4 Resolving multiple non-ghost solutions

The problem of multiple operational and non-operational non-ghost solutions is then sorted out based on topology, singularities, and branching points of the algebraic curves.

2.2.5 Applying power series and analytic continuation

Polynomial elimination techniques will not give clear solutions when applied to the algebraic curve, especially with a very large number of variables. Therefore, the power series of the curve is calculated at point s=0 and then the analytic continuation

technique is used to reach the target point, s=1. If the approximants converge at s=1, then the desired solution is obtained; otherwise, there is no feasible power flow.

3. Analysis of Samples

3.1 Test Systems Description

Four test systems were used in this work, a 4-bus system (Grainger & Stevenson, 1994) in Figure 2, the IEEE 14-bus system in Figure 3, the IEEE 30-bus system in Figure 4 (Christie, 1993; Rajathy, 2011) and the Nigerian 330kV transmission network in Figure 5 (Ayodele et al., 2016). The 4-bus system has 2 generators and 4 lines; the 14-bus system has 5 generators and 20 lines and the 30-bus system has 41 lines and 6 machines. The Nigerian system used in this work has 7 generators, each of which is connected via transformers to the rest of the network, and 31 buses.

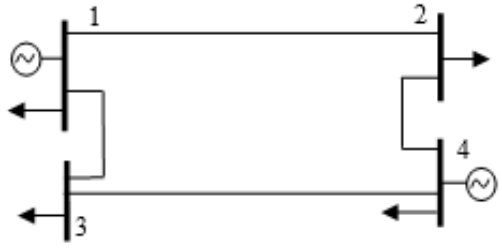

Figure 2: IEEE 4-bus system (Grainger & Stevenson, 1994)

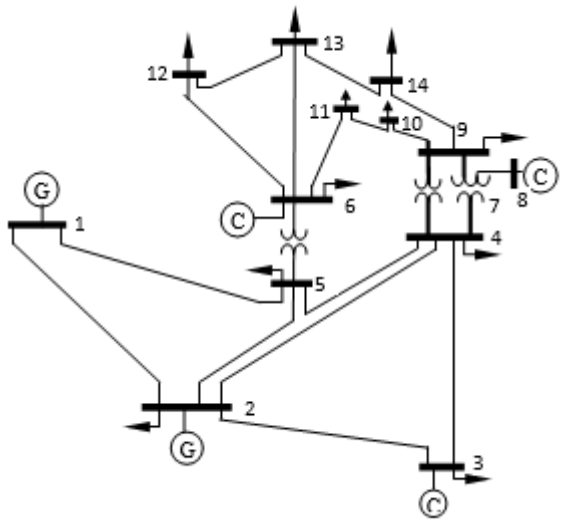

Figure 3: IEEE 14-bus system (Christie, 1993; Appendix A, 2011)

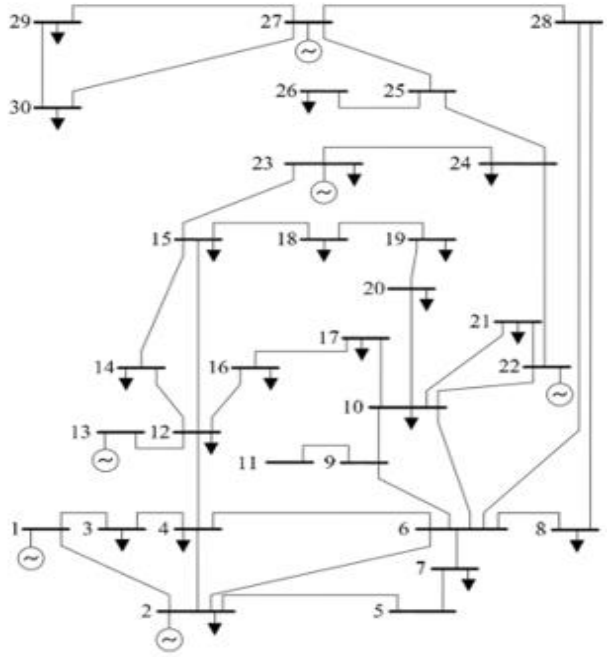

Figure 4: IEEE 30-bus system (Appendix B, 2011; Christie, 1999)

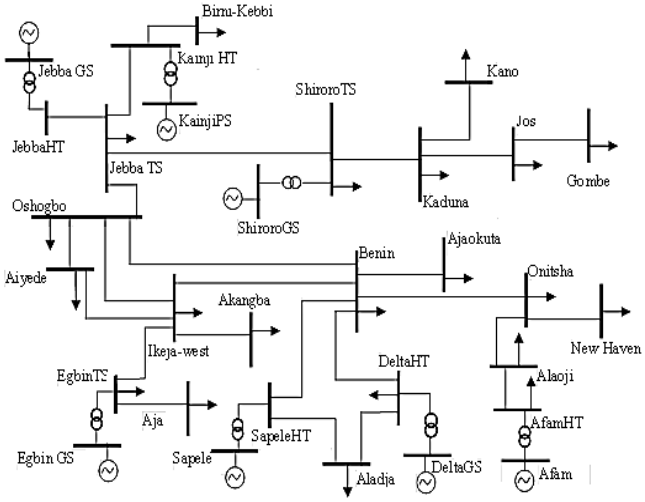

Figure 5: The Nigerian 330kV transmission network (Ayodele et al, 2016)

3.2 Solving the 4-bus system using NRLM

The 4-bus system was analysed where bus 1 is the slack, buses 2 and 3 are the load buses and bus 4 is the generator bus. The net injected powers at bus *i*, P_i^{sch} and Q_i^{sch} at the buses are computed using (18) and (19) where the subscript *g* represents the generated power and *l* the consumed power. From (5) and (6), the real power, P_i^{calc} and reactive power, Q_i^{calc} are calculated for each bus to obtain the results.

$$P_i^{sch}=P_{gi}-P_{li} \quad (18)$$

$$Q_i^{sch}=Q_{gi}-Q_{li} \quad (19)$$

Table 1: Power at the buses

Scheduled power (pu)						Calculated power (pu)					
P_2^{sch}	Q_2^{sch}	P_3^{sch}	Q_3^{sch}	P_4^{sch}	Q_4^{sch}	P_2^{cal}	Q_2^{cal}	P_3^{cal}	Q_3^{cal}	P_4^{cal}	Q_4^{cal}
-1.7	-1.05	-2.0	-1.24	2.38	-0.5	-0.051	-0.62	-0.016	2.93	0.28	0.72

Changes in power after the first iteration by using (21) and (22) are given in (22).

$$\Delta P_i^0=P_i^{sch}-P_i^{cal} \quad (21)$$

$$\Delta Q_i^0 = Q_i^{sch} - Q_i^{cal} \quad (22)$$

$$\begin{bmatrix}\Delta P_2^0\\ \Delta P_3^0\\ \Delta P_4^0\end{bmatrix} = \begin{bmatrix}-1.65\\ -1.98\\ 2.10\end{bmatrix}, \quad \begin{bmatrix}\Delta Q_2^0\\ \Delta Q_3^0\\ \Delta Q_4^0\end{bmatrix} = \begin{bmatrix}-0.43\\ -4.17\\ -1.22\end{bmatrix} \quad (23)$$

3.2.1 Solving the 4-bus system using HELM

Solving the HELM equations (15) - (37) for the four-bus system at s=0 gives the no-load results, where all the bus voltages are equal to $1\angle 0°$. Other power series coefficients are calculated by splitting the left-hand side (LHS) of the equation into real and imaginary parts to give the 8×8 matrix in (23). Details of this can be found in (Subramanian, 2014).

Rows 1 and 2 of the LHS matrix correspond to real and imaginary components of the slack bus equations. Since the slack bus voltage is fixed by taking cognizance of the network topology, the coefficients corresponding to other bus voltages are zero. One more distinct part of the equation is column 7 of the LHS matrix, where all elements are zero except the last row which accounts for the generator bus. The reactive power injected into bus 4, which is a generator bus, is represented by the series term, $Q_4[N]$, consequently, the remaining entries of the column must be zero.

$$\begin{bmatrix} 1 & 0 & 0 & 0 & 0 & 0 & 0 & 0\\ 0 & 1 & 0 & 0 & 0 & 0 & 0 & 0\\ -3.81 & -19.07 & 8.98 & 44.92 & 0 & 0 & 0 & -25.84\\ 19.07 & -3.81 & -44.92 & 8.98 & 0 & 0 & 0 & -5.16\\ -5.16 & -25.84 & 0 & 0 & 8.19 & 40.96 & 0 & -15.11\\ 25.84 & -5.16 & 0 & 0 & -40.96 & 8.19 & 0 & -3.02\\ 0 & 0 & -5.16 & -25.84 & -3.02 & -15.11 & 0 & 40.96\\ 0 & 0 & 25.84 & -5.16 & 15.11 & -3.02 & 1 & 8.19 \end{bmatrix} \begin{bmatrix} V_{1re}[N]\\ V_{1im}[N]\\ V_{2re}[N]\\ V_{2im}[N]\\ V_{3re}[N]\\ V_{3im}[N]\\ Q_4[N]\\ V_{4im}[N] \end{bmatrix}$$

$$= \begin{bmatrix} \delta_{n0}\\ 0\\ \mathrm{Re}\left(S_2^* W_2^*[N-1] - j0.09V_2[N-1]\right)\\ \mathrm{Im}\left(S_2^* W_2^*[N-1] - j0.09V_2[N-1]\right)\\ \mathrm{Re}\left(S_2^* W_2^*[N-1] - j0.10V_3[N-1]\right)\\ \mathrm{Im}\left(S_2^* W_2^*[N-1] - j0.10V_3[N-1]\right)\\ \mathrm{Re}\left(rhs\_Known[N-1]\right)\\ \mathrm{Im}\left(rhs\_Known[N-1]\right) \end{bmatrix} - \begin{bmatrix} 0\\ 0\\ -5.16\\ 25.84\\ -3.02\\ 15.11\\ 8.19\\ -40.96 \end{bmatrix} \quad (23)$$

$$V_{4re}[N] = \delta_{N0} + 0.0202\delta_{N1} - \sum_{n=1}^{N} V_4[n]V_4^*(N-n)]$$

The other elements are a result of separating the admittance matrix into real and imaginary components as in (18). Calculation of right-hand side (RHS) vector for slack bus (rows 1 and 2) and load buses (row 3 to row 6) follows directly from (24) and (25).

$$\sum_{n=1}^{N} Y_{intrans}V_k[N] = S_i^* W_i^*[N-1] - Y_{ishunt}V_i[N-1] \quad (24)$$

$$V_i[N] = \delta_{N0} + \delta_{N1}(V_i^{sp} - 1), \text{ i=slack bus} \quad (25)$$

where rhs_Known[N-1] has coefficients up to degree N-1, that is:

$$rhs\_Known[N-1] = P_i W_i^*[N-1] - j\left(\sum_{n}^{N-1} Q_i[n]W_i^*[N-n]\right) - Y_{ishunt}V_i[N-1] \quad (26)$$

where $W_i(s) = {}^{1}/_{V_i(s)}$ and $V_i(s)$ is the voltage power series for bus i. The solution of the next power series coefficients is obtained by evaluating the RHS of (26). The complex power and inverse voltage series are considered when evaluating load buses, while the reactive power series in (27) and voltage magnitude constraint are involved for generator buses. Equation (27) is then obtained as the solution of the associated linear system of equations.

$$\sum_{n=1}^{N} Y_{intrans} V_n[N] = P_i W_i^*[N-1] - j\left(\sum_{k}^{n-1} Q_i[n] W_i^*[N-n] + Q_i[N]\right) - Y_{ishunt} V_i[N-1] \quad (27)$$

This is followed by determining the Pade approximant of the voltage and reactive power series (Trias, 2012) which uses an asymptotic expansion. Its convergence can be greatly facilitated by appropriate extrapolation measures (Baker, 2012). Calculation of Padé approximants of $V_2(s)$, $V_3(s)$, and $V_4(s)$ series using matrix method can be achieved which yields the results from HELM. The results of the NRLM and HELM for the 4-bus system are shown in Table 2 and Figure 5 in comparison.

3.3 Analyzing the IEEE 14-bus and 30-bus Systems

The NRLM and HELM were applied to the 14-bus and 30-bus benchmark systems in Figures 3 and 4, using Matlab programmes, and the results, the bus voltages, are plotted in Figures 7 and 8.

3.4 Application of NRLM and HELM to the Nigerian System

The Nigerian 330kV transmission grid used as a test system for this study is the 31-bus system in Figure 5. The NRLM and HELM were each applied to the system with the aid of the MATLAB software, though special software was developed by the originator of HELM (Trias, 2012) for the load flow analysis.

4. Results and Discussion

The NRLM is an iterative method and so expectedly, the solution was obtained in each case after some iterations. The HELM produced specific voltage values analytically within the program. The NRLM results for the 4-bus system were obtained in 0.4786 second after 3 iterations, while HELM took 0.0207 second. The plot of the results in Table 2 is shown in Figure 6 where slight differences between the voltage magnitudes of the two methods can be observed. For the 14-bus and 30-bus systems, each converged after 7 iterations with NRLM; voltage values are plotted in Figures 7 and 8 respectively showing barely any difference between the voltages obtained from the two methods.

For the Nigerian 330kV transmission system, the NRLM required five iterations to converge but was still slower than HELM. From the plots of the two methods in Figures 9 and 10, it is obvious that the results of the two methods are quite different. The computation times and iterations of all the test systems are summarized in Table 3 where HELM is seen to conclude the computations faster than NRLM in all cases.

Table 2: The 4-bus system voltage magnitudes

Bus No.	NRLM	HELM
1	1.0000	1.0000
2	0.9451	0.9280
3	0.9475	0.9357
4	0.9700	0.9455

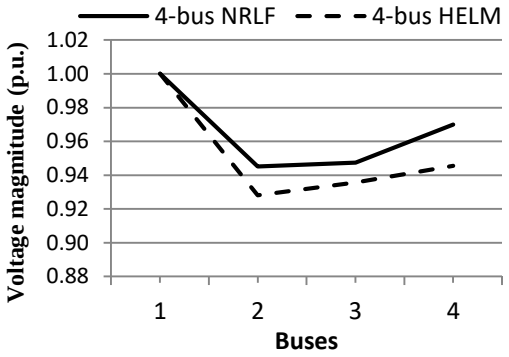

Figure 6: NRLM and HELM for the 4-bus system

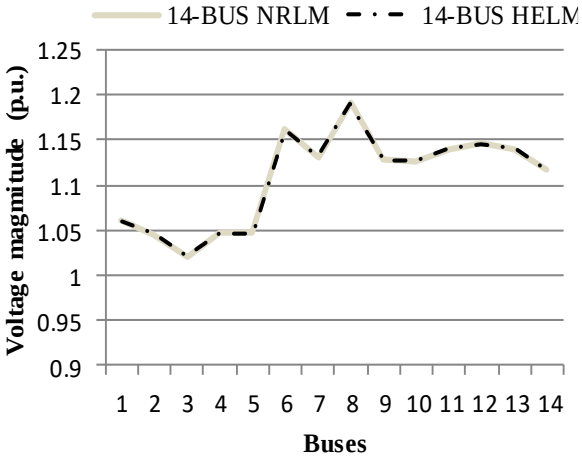

Figure 7: NRLM and HELM for the 14-bus system

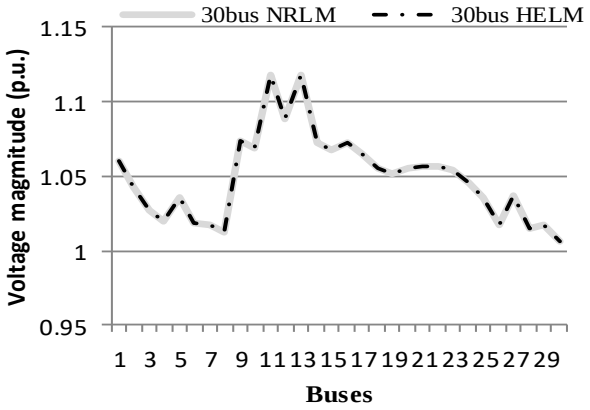

Figure 8: NRLM and HELM for the 30-bus system

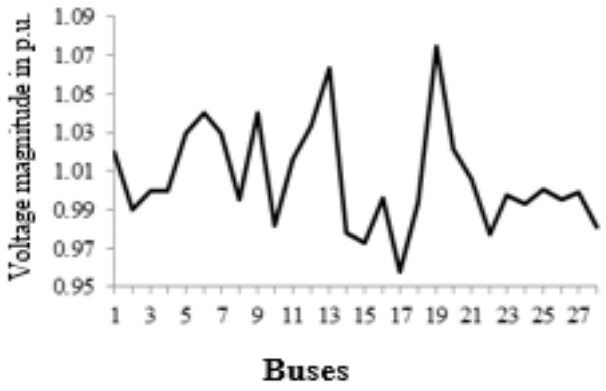

Figure 9: NRLM result for 330kV network

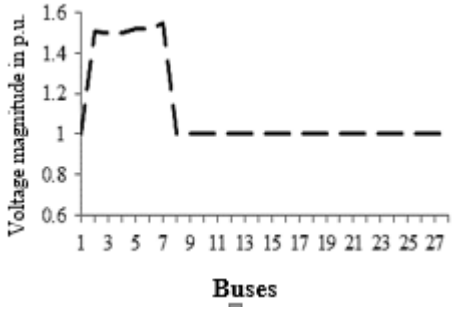

Figure 10: HELM result for 330kV network

The voltage values obtained for the Nigerian 330kV transmission system using NRLM vary from 0.96-1.04 p.u, which is slight but scattered on the graph though this is typical of some load flow results.

The voltage values from HELM vary from 1.0000-1.5453 p.u. which could confirm the fact that though HELM can produce results faster, the precision is lower than that of iterative algorithms (Sauter, 2017). Another reason could be because HELM can signal a potential voltage collapse or lack of solution (Black, 2012; Trias, 2012) which is not feasible with iterative methods. The Nigerian system has insufficient capacity and is generally agreed to be weak. (Bakare, *et al.*, 2007; Amoo, 2013; Adaramola, *et al*., 2011; Gujba, et al, 2010; Onojo, *et al*., 2013; Onohaebi & Apeh, 2007). This makes it susceptible to voltage instability and voltage collapse and could account for the unusual results.

Table 3: Solution times of sample networks

CASE STUDIES	Time in seconds		Percentage reduction in analysis time with HELM	No of iterations for NRLM
	NRLM	HELM		
4-bus system	0.4786	0.0207	95.7%	3
14-bus system	0.3354	0.0912	72.8%	7
30-bus system	0.5755	0.0885	84.6%	7
Nigerian 330kV network	1.1249	0.2181	80.6%	5

5. Conclusion

This work was able to explore the complexities of the HELM algorithm and infer from the analysis that it is faster than NRLM. The results for the standard IEEE bus systems are very close. The Nigerian 330kV, 31-bus system, not found to have been analysed with HELM before, showed a result pattern that is quite different compared to NRLM. Since HELM can give indication of voltage collapse in a system, unlike NRLM, the state of the system is a likely cause of the result obtained with HELM. Also, the software specially produced for HELM by Trias (2012) could be its best tool until the method fully evolves and other types of software could be employed effortlessly. HELM's accuracy in terms of actual results is said to be lower than the NRLM, but further analytical evidence is required to establish this fact.

References

Appendix A. (2011). Retrieved April 7, 2022, from DATA SHEETS FOR IEEE 14 BUS SYSTEM: http://shodhganga.inflibnet.ac.in/bitstream/10603/5247/18/19_appendix.pdf.

Appendix B. (2011, April). Retrieved April 7, 2022, from Shodhganga@INFLIBNET: shodhganga.inflibnet.ac.in/bitstream/10603/5247/18/19_appendix.pdf

Adaramola, M. S., Paul, S. S., & Oyedepo, S. O. (2011). Assessment of electricity generation and energy cost of wind energy conversion systems in north-central Nigeria. *Elselvier, Energy Conversion and Management, vol. 52*, 3363–3368.

Amoo, A. L. (2013). Harmonic Power Flow in Nigerian Power System with PV Site. (pp. 319-323). Langkawi, Malaysia: PEOCO.

Ayodele, T. R., Ogunjuyigbe, A. S. O. & Oladele, O. O. (2016). Improving the Transient Stability of Nigerian 330kV Transmission Network Using Static VAR Compensation Part I:The Base Study. *Nigerian Journal of Technology (NIJOTECH), 35(1)*, 155 – 166.

Bakare, G. A., Krost, G., Venayagamoorthy, G. K. & Aliyu, U. O. (2007). Differential Evolution Approach for Reactive Power Optimization of Nigerian Grid System., (pp. 1-6).

Baker, G. A. (2012). Pade Approximant. *Scholarpedia 7(6)*, 9756.

Black, J. (2012). *Utilizing HELM™ for Advanced Grid Management and Planning.* Retrieved January 15, 2012, from http://energytech2012.org/wp-content/uploads/2012/05/W-S1-D-Battelle_EnergyTech2012_HELM_JBlack.pdf

Cai, J. and Mitra, N. (2012). Analytics for Steady State Operation of Autonomous Microgrid. *In Power and Energy Society General Meeting, 2012 IEEE*, (pp. 1-5).

Christie, R. (1993, August). *Power Systems Test Case Archive*. Retrieved April 7, 2022, from labs.ece.uw.edu: https://labs.ece.uw.edu/pstca/

Christie, R. D. (1999, August). *30 Bus Power Flow Test Case*. Retrieved April 7, 2022, from Power Systems Test Case Archive: https://labs.ece.uw.edu/pstca/pf30/pg_tca30bus.htm

Grainger, J. J. & Stevenson, W.D. (1994). *Power Systems Analysis.* New: McGraw-Hill.

Gujba, H., Mulugetta, Y. & Azapagic, A. (2010). Environmental and economic appraisal of power generation capacity expansion plan in Nigeria. *Elselvier: Energy Policy, vol. 38*, 5636–5652.

Hiskens, I. A. (2003). *Power Flow Analysis.* Madison.

Huneault, M. and Galiana, F. D. (1991). A Survey of the Optimal Power Flow Literature. *IEEE Transactions on Power Systems, 6*(2), 762-770.

Kalantari, A., Kouhsari, S. M. and Rastegar, H. (2003). Piecewise Fast Decoupled Load Flow Using Large Change Sensitivity. *IEEE Power Engineering Society General Meeting, 2*, 957– 961.

Mehta, D., Mohlzahn, D. K., & Turitsyn, K. (2016, July). Recent Advances in Computational Methods for the Power Flow Equations. *American Control Centre, 6*(8), 1-13.

Metha, V. K. & Metha, R. (2017). *Priciples of Power Systems.* S. Chand.

Ogbuefi, U. and Madueme, T. (2015). A Power flow analysis of the Nigerian 330kV Electric Power System. *IOSR JEEE, 10(1)*, 46-57.

Olobaniyi, F. (2015). *Diakoptic Assessment of Power System Voltage Variations and Applications in Weak Grids Introduced by Wind Energy – The Nigerian Power System in Perspective (Thesis)* . Bristol: University of the West of England.

Onohaebi, O. S. and Apeh, S. T. (2007). Voltage Instability In Electrical Network:A Case Study of the Nigerian 330kV Transmission Grid. *Research Journal of Applied Sciences, 2*(8), 865-874.

Onojo, O. J., Onoiwu, G. C. & Okozi, S. O. (2013). Analysis of Power Flow Of Nigerian 330kv Grid System (Pre and Post) Using Matlab. *EJNAS, 1(2)*, 59-66.

Rajathy, R. (2011, April). *Investigations on Power System Operation and Management in Restructured Market*. Retrieved April 7, 2022, from Shodhganga@INFLIBNET: http://hdl.handle.net/10603/5247

Rao, S. F. (2016). The Holomorphic Embedding Method Applied to the Power-Flow Problem. *IEEE Transactions on Power Systems, 31(5)* , 3816-3828.

Sauer, P. (1981). Explicit Load Flow Series Functions. *IEEE Transactions on Power System Apparatus, PAS-100*(8), 3754-3763.

Sauter, P. S. (2017). Comparison of the Holomorphic Embedding Load Flow Method with Established Power Flow Algorithms and a New Hybrid Approach. *2017 Ninth Annual IEEE Green Technologies Conference* (pp. 203-210). IEEE.

Subramanian, M. K. (2014). *Application of Holomorphic Embedding to the Power Flow Problem.*

Theraja, B. I. and Theraja, A. K. (2012). *Electrical Technology* (24th ed., Vol. III). Ram Nagar, New Delhi, India: S Chand & Company Ltd.

Trias, A. (2012). The Holomorphic Embedding Load Flow Method. *Power and Energy Society General Meeting* (pp. 1-8). IEEE.

Trias, A. (2012). *Two Bus Model Detail.* Retrieved February 24, 2017, from http://www.gridquant.com/assets/two-bus-model-detail.pdf

Trias, A. (2015). Fundamentals of the Holomorphic Embedding Load Flow Method. *IEEE PES General Meeting*, 1-17.

Xu, W., et al. (1998, May). Series Load Flow: A Novel Non-Iterative Load Flow Method. *IEEE Proceedings on Generation Transmission and Distribution, 145*(3), 251-256.